Quantum transitions in ^{3}He adsorbed on carbon nanotube

I. Todoshchenko[1,*], M. Kamada[1], J.-P. Kaikkonen[1], Y. Liao[2], A. Savin[1], M. Will[1], E. Sergeicheva[1], T. S. Abhilash[1], E. Kauppinen[2], and P.J. Hakonen[1,*]

[1] *Low Temperature Laboratory, Department of Applied Physics, Aalto University, 00076 Aalto, Finland*

[2] *Nano Materials Group, Department of Applied Physics, Aalto University School of Science, 00076 Aalto, Finland*[*]

(Dated: March 27, 2026)

[*] igor.todoshchenko@aalto.fi, pertti.hakonen@aalto.fi

Supplementary Information

I. Matrix elements of longitudinal transitions

In the main text we have calculated matrix elements of longitudinal transitions using the potential of the particle calculated from kinetics of a particle oscillating with the tube,

$$V(x,t) = \frac{\Omega^2 h_0^2 m}{2} \sin^2 \frac{\pi x}{L} \cos^2 \Omega t, \tag{1}$$

where h_0 and Ω are amplitude and frequency of the oscillations of the nanotube. The probability of longitudinal quantum transition of the particle is proportional to square of the matrix element

$$V_{NK}(t) = (1/2)\Omega^2 h_0^2 m \big\langle N \big| \sin^2(\pi x/L) \big| K \big\rangle \cos^2 \Omega t, \tag{2}$$

which gives the selection rules $K = N \pm 2$ due to symmetry of the longitudinal wavefunctions $\psi_N = \sin \pi N x/L$, $\psi_K = \sin \pi K x/L$.

Alternatively, one may consider longitudinal transitions directly from particle-tube interaction. In this case potential energy of the particle is oscillating, $U(\vec{r},t) = U_0\big(r + h_0 \sin(\pi x/L) \cos \Omega t \cos \phi\big)$ where $U_0(r)$ is the adsorption potential, $h = h_0 \sin(\pi x/L) \cos \Omega t$ is the shape of the oscillating tube, and ϕ is the orbital angle. For a small oscillations we expand the oscillating potential as

$$U(r,x,\phi,t) = U_0(r) + \frac{dU_0}{dr} h_0 \sin \frac{\pi x}{L} \cos \Omega t \cos \phi + \frac{1}{2} \frac{d^2 U_0}{dr^2} h_0^2 \sin^2 \frac{\pi x}{L} \cos^2 \Omega t \cos^2 \phi. \tag{3}$$

The first term $U_0(r)$ does not depend on the longitudinal coordinate x and therefore gives zero contribution to any of matrix elements of longitudinal transitions $\big\langle nlN \big| U \big| nlK \big\rangle$ where n and l are the radial and orbital quantum numbers. The second, linear term contains $\cos \phi$, and the corresponding diagonal orbital matrix element $\big\langle l \big| \cos \phi \big| l \big\rangle$ is zero. Transitions between different orbital levels have much higher energies than the longitudinal transitions and therefore are left aside from the present consideration.

Matrix element of the quadratic term gives, after integration over r and ϕ,

$$U_{NK}(t) = \frac{1}{4}\Big\langle \frac{d^2U_0}{dr^2} \Big\rangle_n h_0^2 \big\langle N\big| \sin^2 \frac{\pi x}{L} \big|K\big\rangle \cos^2 \Omega t. \tag{4}$$

Both two matrix elements of perturbing potential, $V_{NK}(t)$ in Eq. (2) and $U_{NK}(t)$ in Eq. (4) contain an identical core $\big\langle N\big| \sin^2 \pi N x/L \big|K\big\rangle \cos^2 \Omega t$ representing the square of the shape of the oscillating tube. However, the first approach assumes that the particle is oscillating with the tube, while in the second approach particle resides at rest, but the adsorption potential induced by the tube is oscillating around it. The prefactors in Eq. (2) and Eq. (4) accordingly represent a kinetic energy of helium particle oscillating with the tube, and a potential energy of immobile particle in the oscillating potential. As the frequency of oscillations of the tube is many orders of magnitude lower than the frequency of radial motion of the particle in the adsorption potential, we assume that there is no, or very weak lagging of the particle behind the tube. However, both opposing approaches give the same selection rules and the same relative amplitudes of longitudinal transitions.

II. Atomic quantum fluctuations in the radial direction

If the population of the first layer is small, no significant zero-point pressure is applied to an individual helium atom which can be thus considered as a single particle in the adsorbing potential of carbon nanotube. However, due to quantum fluctuations in the transverse direction, atoms can be thrown from the first layer to the excited levels. Quantum fluctuations are known to be responsible for zero-point noise currents [18], for zero-point oscillations of helium liquid-solid interfaces [19], for zero-point quasiparticles in degenerate Fermi liquids [18], and for zero-point spin reduction in low-dimensional antiferromagnets [20]. More generally, the famous fluctuation-dissipation theorem states that any physical quantity x has non-zero amplitude of fluctuations even at absolute zero.

The probability of a single ^{3}He particle to occupy the second radial layer can be directly estimated by using Fluctuation-dissipation theorem,

$$\langle (z - \overline{z})^2 \rangle = \frac{\hbar}{\pi} \int \chi''(\omega) \coth \frac{\hbar\omega}{2T} d\omega, \tag{5}$$

where $\chi \equiv z/f$ is the susceptibility of the coordinate with respect to the conjugated force $f = E/z$. To find the susceptibility $\chi(\omega)$ we consider a time evolution of the wavefunction, and

the corresponding average distance $\langle z\rangle$ of a particle from the surface of nanotube, induced by the "probe force" $f_z(t) = f_0 \cos\omega t$ which generates a perturbation potential $\hat{V}(t) = -(z - z_{11}^{(0)}) f_0(e^{i\omega t} + e^{-i\omega t})/2$ where $z_{11}^{(0)} \approx 0.27$ nm is average distance from the tube in the radial ground state. As $z_{11}^{(0)}$ and $z_{22}^{(0)}$ are much smaller than the diameter of the tube, we can neglect the curvature of the tube. In the framework of the perturbation theory [12] the wavefunction of the particle can be approximated as $\Psi_n(z,t) = \sum a_{kn}(t)\psi_k^{(0)}(z)e^{-i(E_k/\hbar)t}$ where $\psi_k^{(0)}(z)$ are stationary eigen wavefunctions of the unperturbed adsorption Hamiltonian. Assuming that the particle is near the first level, we may write $a_{11}(t) \simeq 1 + a_{11}^{(1)}(t)$, $a_{k1}(t) \simeq a_{k1}^{(1)}(t)$, where first-order corrections $|a_{k1}^{(1)}(t)| \ll 1$. Application of the perturbation potential results in the evolution of the of the expansion coefficients, $da_{k1}^{(1)}/dt = (-i/\hbar\,)V_{k1}(t) - a_{k1}^{(1)}/\tau_{k1}$ where $1/\tau_{k1}$ is relaxation rate from the level k to the initial state 1. By integrating the perturbation term, we find $a_{k1}^{(1)}(t) = -(i/\hbar)e^{-t/\tau_{k1}} \int V_{k1}(z,t)e^{t/\tau_{k1}}dt$. Matrix elements $V_{k1}(t)$ are found by integration over the coordinate space with time-dependent zero-order wavefunctions, $V_{k1}^{(0)}(t) = \int e^{iE_k t/\hbar}\psi_k^{(0)*}\hat{V}e^{-iE_1 t/\hbar}\psi_1^{(0)}dz = -e^{i\omega_{k1}t}f_0(z_{k1}^{(0)} - z_{11}^{(0)})(e^{i\omega t} + e^{-i\omega t})/2$. Finally, we obtain

$$a_{k1}^{(1)}(t) = \frac{f_0(z_{k1}^{(0)} - z_{11}^{(0)})}{2\hbar}\Big(\frac{e^{i(\omega_{k1}+\omega)t}}{\omega_{k1} + \omega - i/\tau_{k1}} + \frac{e^{i(\omega_{k1}-\omega)t}}{\omega_{k1} - \omega - i/\tau_{k1}}\Big). \tag{6}$$

The perturbation-induced evolution of the ground-state wave-function of the particle is written, in the first-order corrections, as $\Psi(t) \simeq [1 + a_{11}^{(1)}(t)]\Psi_1^{(0)}(t) + \sum_{k\neq 1} a_{k1}^{(1)}(t)\Psi_k^{(0)}(t)$, and the expectation value of the coordinate of the particle is

$$z(t) = \int \Psi^*(t) z \Psi(t) dz \simeq z_{11}^{(0)} + \sum_{k\neq 1} a_{k1}^{(1)}(t)e^{-i\omega_{k1}t}z_{k1}^{(0)} + \sum_{k\neq 1} a_{k1}^{(1)*}(t)e^{i\omega_{k1}t}z_{k1}^{(0)*} = z_{11}^{(0)} +$$
$$\frac{f_0}{\hbar} z_{k1}^{(0)}(z_{k1}^{(0)} - z_{11}^{(0)})\Big[\frac{(\omega_{k1}+\omega)\cos\omega t - (1/\tau_{k1})\sin\omega t}{(\omega_{k1}+\omega)^2 + 1/\tau_{k1}^2} + \frac{(\omega_{k1}-\omega)\cos\omega t + (1/\tau_{k1})\sin\omega t}{(\omega_{k1}-\omega)^2 + 1/\tau_{k1}^2}\Big], \tag{7}$$

where $z_{ik}^{(0)} = \int \psi_i^{(0)*} z \psi_k^{(0)} dz$ are matrix elements of the coordinate in the basis of non-perturbed stationary wave functions.

Imaginary part of the susceptibility is found by dividing amplitude of the out-of-phase term in Eq. (7) by the amplitude of the probing force f_0,

$$\chi'' = \frac{1}{\hbar}\sum_{k\neq 1} \frac{z_{k1}^{(0)}(z_{k1}^{(0)} - z_{11}^{(0)})}{\tau_{k1}}\Big[\frac{1}{(\omega_{k1}-\omega)^2 + 1/\tau_{k1}^2} - \frac{1}{(\omega_{k1}+\omega)^2 + 1/\tau_{k1}^2}\Big], \tag{8}$$

and the amplitude of fluctuations of coordinate (5) is then

$$\overline{(z-z_{11}^{(0)})^2}=\sum_{k\neq 1}\frac{z_{k1}^{(0)}(z_{k1}^{(0)}-z_{11}^{(0)})}{\pi\tau_{k1}}\int_0^\infty\left[\frac{\coth(\hbar\omega/2T)d\omega}{(\omega-\omega_{k1})^2+1/\tau_{k1}^2}-\frac{\coth(\hbar\omega/2T)d\omega}{(\omega+\omega_{k1})^2+1/\tau_{k1}^2}\right]. \qquad (9)$$

In the limit of the *weak relaxation*, $\omega_{k1}\tau_{k1}\gg 1$, the first integral in Eq. (9) is dominating due to the resonant behavior at $\omega\approx\omega_{k1}$. Furthermore, most of the contribution to the integral is situated near the resonance $\omega\sim\omega_{12}$, and at temperatures $T\ll\hbar\omega_{k1}\sim 50$ K cotangent can be replaced with 1. The amplitude of fluctuations (9) is then calculated analytically,

$$\overline{(z-z_{11}^{(0)})^2}\simeq\frac{1}{\pi}\sum z_{k1}^{(0)}(z_{k1}^{(0)}-z_{11}^{(0)})(\frac{\pi}{2}+\arctan\omega_{k1}\tau_{k1})\simeq\sum z_{k1}^{(0)}(z_{k1}^{(0)}-z_{11}^{(0)}). \qquad (10)$$

Amplitude of fluctuations does not depend either on $\omega_{k1}=(E_k-E_1)/\hbar$, or on the relaxation time τ. Normalized spectral density of fluctuations in the low-dissipation case of two-level potential is shown at Fig S1(a). Clearly, the amplitude of the resonance is inversely proportional to the width $1/\tau$, and the integral does not depend on τ. Using the adsorption potential for a helium atom on carbon lattice [14] we have calculated the first two wavefunctions $\psi_1(z)$ and $\psi_2(z)$ as shown in Fig. 3 of the main text, and calculated matrix elements $z_{11}^{(0)}=2.9$ Å, $z_{22}^{(0)}=3.6$ Å, and $z_{21}^{(0)}=-0.28$ Å. The fluctuation amplitude $\sqrt{\langle(z-z_{11}^{(0)})^2\rangle}=0.94$ Å is, as expected, much larger than the width of the ground-state wavefunction, $\sqrt{\int\psi_1^*(z)(z-z_{11})^2\psi_1(z)dz}=0.31$ Å.

We should remember that the susceptibility χ was calculated in the framework of the perturbation theory which is not applicable when coefficients a_{ki} become large. However, the conclusion of high probability of occupying excited levels remains correct if the assumption of small a_{ik} breaks. It is, in fact, an obvious result: the absence of dissipation means that the particle doesn't interact with the surroundings and consequently doesn't possess temperature of the bath. Energy of the particle, generally, does not have to be conserved. The particle may exist in the mixed state and oscillates between stationary levels with the frequencies ω_{ki}. The particular state is determined not by the thermodynamics but rather by the history: how exactly the particle was trapped in the potential well.

The requirement of low dissipation, $\omega\tau\gg 1$, is not demanding at low densities. It simply means that during the period of one evolution there will be no inelastic scattering on other particles or phonons, or on longitudinal profile of the potential. At low temperatures the

number of phonons is very small, and interaction of the particle with the boundaries where the wavefunction vanishes is also very weak. At the same time, all radial frequencies are very high, $\omega_{ki} \sim 10^{13}$ rad/s, and if there are no, or very little amount of other particles on the tube, the dissipation is always low. Hereof, a process in which free initially particle loses its energy to be trapped in the adsorption potential is very slow if the dissipation is low. Indeed, in our experiment we had to wait about one day for a new configuration to settle down after every adding of helium to the cell, which proves the low dissipation assumption.

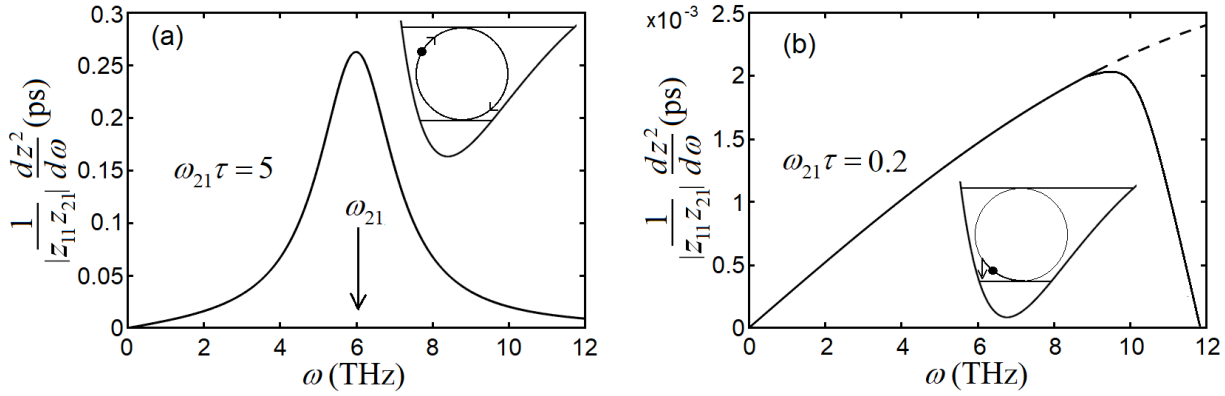

Fig. S1 Normalized spectral density of quantum fluctuations for the potential with two levels, calculated with Eq. 9. (a) Low dissipation, $\tau \gg 1/\omega_{12}$. Fluctuations have a sharp resonance at $\omega = \omega_{21} = (E_2 - E_1)/\hbar$. The integral is of the order of 1. Insert: illustration of the evolution of the particle between two stationary levels. (b) Strong dissipation and absence of resonance. Fluctuations are suppressed, having an integral on the order of $(8/\pi)(\omega_{21}\tau)^3 \ll 1$. The high frequency cutoff corresponds to one-way traveling time of the particle on the stationary level. Insert: illustration of fast relaxation of the particle to the ground-state level.

At $\tau \to \infty$ the expression in Eq. (6) for perturbation coefficients $a_{k1}(t)$ turns to equation (40.9) in Ref. [12] for the case of zero dissipation. However, a finite relaxation time introduced here provides the smallness $a_{k1}(t) \ll 1$ even at $\omega \to \omega_{k1}$ if a probe force is small enough, while in the dissipationless case a_{k1} goes to infinity at the resonance with any finite force [12]. Finite dissipation thus ensures that the susceptibility $\chi(\omega)$ is finite in the whole range $0 < \omega < \infty$, and that the FDT-integral converges.

In the case of *strong dissipation* the relaxation time is short, $\omega\tau \ll 1$, and Eq. (9) is simplified by decomposition $[(\omega \pm \omega_{k1})^2 + 1/\tau_{k1}^2]^{-1} \simeq \tau_{k1}^2 - \tau_{k1}^4(\omega \pm \omega_{k1})^2$:

$$\overline{(z-z_{11}^{(0)})^2} \simeq \frac{4}{\pi}\sum z_{k1}^{(0)}(z_{k1}^{(0)}-z_{11}^{(0)})\tau_{k1}^3\omega_{k1}\int_0^\infty \omega d\omega \simeq \frac{8}{\pi}\sum z_{k1}^{(0)}(z_{k1}^{(0)}-z_{11}^{(0)})\tau_{k1}^3\omega_{k1}\omega_1^2, \quad (11)$$

where we again have replaced cotangent with unity, as most of the integral is situated at high frequencies. The integral diverges, and the cut-off frequency has been introduced, see Fig S1(b). Obviously, the fastest process in the system is traveling time at the ground state, and therefore, natural cutoff frequency is $\omega_{cut} \sim 2\omega_1 = E_1/\hbar$. In contrast to the weak relaxation limit, the estimation of the fluctuations in the strong relaxation case is correct even quantitatively, as we always remain in the framework of the perturbation theory, $a_{k1}(t) \ll 1$. Magnitude of radial fluctuations in the strong dissipation case is lower by the factor of $(8/\pi)\omega_{12}\omega_1^2\tau^3$ than in the low dissipation case.

III. Fluctuating charge

An alternative explanation of the side peaks is a change of resonant frequency due to the fluctuations of the background charge, in which excess electrons/holes may occasionally be trapped in the oxide layer on the gate electrode below the tube, or on the tube itself. The resonant frequency changes due to an additional electrostatic force which deforms the tube and therefore changes its spring constant. In its turn, mechanical sagging of the tube modifies its electrical capacitance. Mutual coupling of mechanical and electrical degrees of freedom in nano-oscillators has been introduced by Bachtold and colleagues [21], and here we discuss the electro-mechanical coupling in more details and give more quantitative description to it.

When a DC voltage U_g is applied to the gate electrode, the tube acquires an electrical charge $Q = Q_{tube}$. The balance of electrical potentials and charges is shown in Fig. S2(a). The charge Q is set by the balance of potentials $U_{tube} = U_g - Q_g/C_g = (Q+Q_g)/C_{tube}$, $Q = C_{tube}U_g - Q_g(C_g + C_{tube})/C_g$. Here $C_g = 2\pi\varepsilon_0 L/\ln 2H/r_0$ is the tube–gate capacitance, and $C_{tube} = 2\pi\varepsilon_0 L/\ln 2\mathcal{L}/r_0$ is the capacitance of the tube with respect to cell walls. Our tube has radius $r_0 = 0.8$ nm, length $L = 700$ nm, and placed at the distance $H = 300$ nm from the gate and at the distance $\mathcal{L} \simeq 3$ mm to the nearest wall, which gives $C_g = 5.9{\cdot}10^{-18}$ F and $C_{tube} = 2.5\cdot 10^{-18}$ F. By minimizing the total electrical energy $\mathcal{E} = C_g(U_g - U_{tube})^2/2 + C_{tube}U_{tube}^2/2 = Q_g^2/2C_g + (C_{tube}/2)(U_g - Q_g/C_g)^2$, we find $\overline{Q_g} = C_g C_{tube}U_g/(C_g + C_{tube})$. $\overline{Q_g}$

denotes the value of charge on the gate which formally minimizes the total electrical energy. However, due to the quantization of charge $Q_g = N \cdot \overline{e}$, the real charge Q_g differs from $\overline{Q_g} = C_g C_{tube} U_g/(C_g + C_{tube})$ by an amount of $\Delta Q = Q_g - \overline{Q_g}$.

The total electrical energy, including the Coulomb blockade energy, can therefore be expressed as a function of the gate voltage U_g and of the excess charge ΔQ:

$$\mathcal{E}(U_g, \Delta Q) = \frac{C_g + C_{tube}}{2C_g C_{tube}} Q_g^2 = \frac{C_g + C_{tube}}{2C_g C_{tube}} \Big(\frac{C_g C_{tube}}{C_g + C_{tube}} U_g + \Delta Q \Big)^2. \tag{12}$$

As energy at certain U_g has a minimum at $\Delta Q = 0$, a switching $\Delta Q \rightarrow \Delta Q \mp \overline{e}$ with trapping/escaping of an electron to/from the tube occurs when $\mathcal{E}(U_g, \Delta Q) = \mathcal{E}(U_g, \Delta Q \pm \overline{e})$, or, at $\Delta Q = \pm\overline{e}/2$, so that $\Delta Q = \{-\overline{e}/2 \ ... \ \overline{e}/2\}$. The Coulomb-blockade modulation period of the gate voltage is $\Delta U_g = (C_g + C_{tube})\overline{e}/C_g C_{tube} = 92$ mV which is in very good agreement with the measured oscillations of the trans-conductance dI/dU_g, see Fig. S2(b). Trans-conductance of the tube depends on the potential $U_{tube} = Q_g/C_{tube}$ which is modulated with the periodicity ΔU_g.

Electrical energy (12) depends on the capacitances C_g and C_{tube} which in turn depend on a deflection of the tube h, which is the origin of the electro-mechanical coupling [21]. The electrical force acting on the tube is then

$$f_e = -\frac{\partial \mathcal{E}}{\partial h} = -\Big(U_g + \frac{\Delta Q}{C} \Big) \cdot \frac{\partial \Delta Q}{\partial h}, \tag{13}$$

where $C = C_g C_{tube}/(C_g + C_{tube})$, and $\partial \Delta Q/\partial h = -C_h^{'} U_g$. The force can be represented in the form $f_e = -k_e h = (\partial f/\partial h)h$, where

$$k_e = -\frac{\partial f_e}{\partial h} = \Big(U_g + \frac{\Delta Q}{C} \Big) \frac{\partial^2 \Delta Q}{\partial h^2} + \frac{1}{C} \Big(\frac{\partial \Delta Q}{\partial h} \Big)^2 = \Big[\frac{(C_h^{'})^2}{C} - C_{hh}^{''} \Big] U_g^2 - \frac{C_{hh}^{''}}{C} U_g \Delta Q. \tag{14}$$

The Coulomb-blockade-modulated part of the electrical spring constant is $k_e^{\sim} = -(C_{hh}^{''}/C) \cdot U_g \Delta Q$. The electrical spring constant contributes to the mechanical spring constant $k = k_m + k_e^{\sim}$, and the Coulomb-modulated contribution to the spring constant is maximal (minimal) when $\Delta Q = \pm\overline{e}/2$: $k_e^{\sim}(\pm\overline{e}/2) = \mp C_{hh}^{''} U_g \overline{e}/2C$.

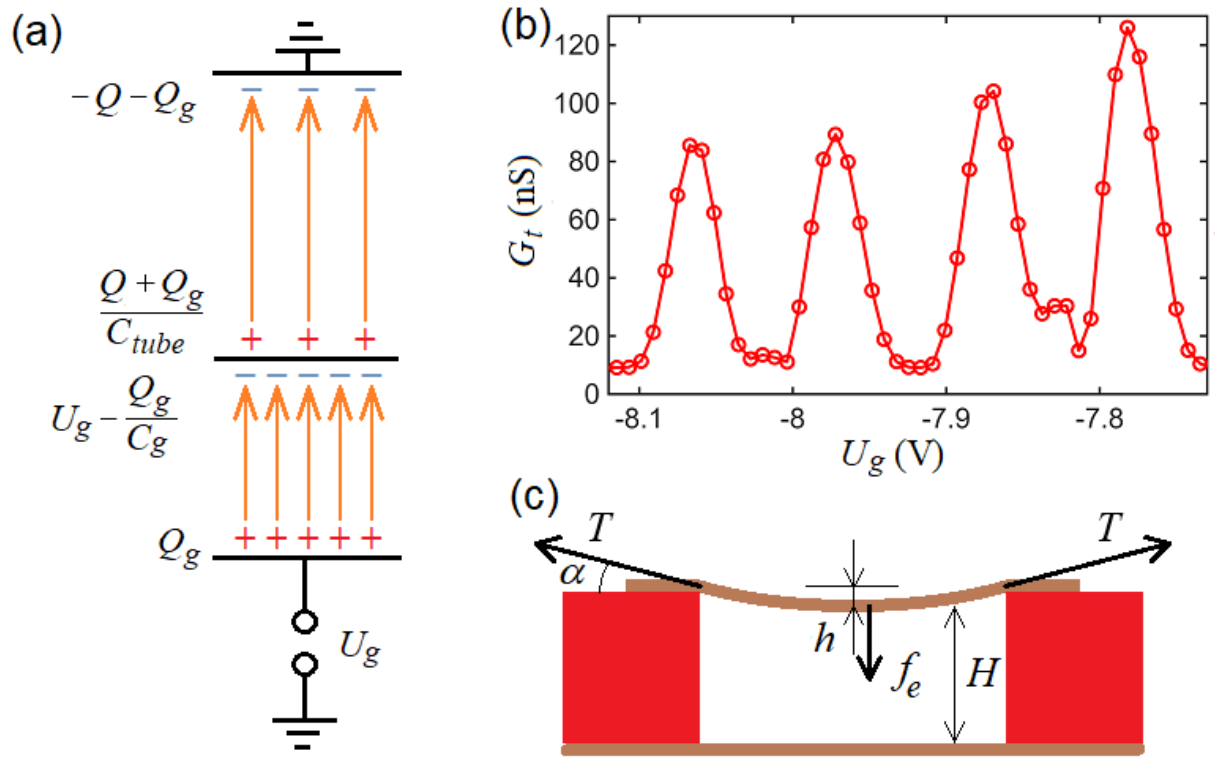

Fig.S2 Electro-mechanical coupling in the nanotube. (a) Potentials and charges on the gate and on the tube. As the tube is conducting, its potential calculated from the distant ground, $(Q+Q_g)/C_{tube}$, is equal to the potential calculated from the gate, $U_g - Q_g/C_g$. Q is determined by minimizing the total electrical energy, see text. (b) Example of measured trans-conductance dI/dU_g as a function of the gate voltage U_g at constant bias voltage of 5 mV *vs.* gate voltage. The observed periodicity of the trans-conductance due to Coulomb-blockade modulation is very close to the expected value $\Delta U_g = (C_g + C_{tube})\overline{e}/C_{tube}C_g = 92$ mV. (c) Sketch of the forces and deformation of the tube.

The mechanical spring constant $k_m = f/h$ is calculated from the force and sagging balances $f = 2T\alpha$ (α is the sagging angle) and $h = \alpha L/4$, see Fig. S2(c). As the average sagging of parabolically shaped tube $\overline{h}$ is close to the maximum sagging, $\overline{h} = (2/3)h$, we can ignore the geometrical factor in estimation of spring constants. Then $k_m = f_m/h = 8T/L$ where the tension of the tube T is calculated from the resonance frequency F_0 and the mass density $\mu = M/L \approx 3.9 \cdot 10^{-15}$ kg/m as $T = 4F_0^2L^2\mu = 8 \cdot 10^{-10}$ N, and the mechanical spring constant is then $k_m \approx 10^{-3}$ N/m. Finally, we can find the amplitude of modulation of the resonant frequency due to electro-mechanical coupling,

$$\frac{\Delta F_0{}^{em}}{F_0} = \frac{k_e^{\sim}(\overline{e}/2) - k_e^{\sim}(-\overline{e}/2)}{2k_m} = -\frac{(C_{hh}^{''}/C)U_g\overline{e}L}{16T}. \tag{15}$$

For our dimensions, $C_{hh}^{''}/C \approx 10^{12}$ 1/m^2, and modulation of the electrical spring constant is $\Delta k_e^{\sim} = (C^{''}/C)U_g\overline{e} \sim 1.5 \cdot 10^{-6}$ N/m $\approx 0.0015\ k_m$. The corresponding modulation of the resonant frequency is $\Delta F_0 \approx 0.0007 F_0 = 0.25$ MHz. An additional electron tunneled to the tube or to the isolation of the gate electrode will change the potential of the tube by an amount of $\overline{e}/C_{tube}$ and shift the resonance by the same amount $\Delta F \sim 0.25$ MHz as the switch $\Delta Q \to \Delta Q + \overline{e}$.

The estimated value of the frequency shift due to fluctuating background charge is very close to the observed separations of side peaks, and larger quantized shifts would correspond to two, three, etc. electrons. Despite the distribution of traps for electrons being arbitrary, capture of additional charge redistributes other charges to a uniform pattern, and potentials will change by the same amount no matter where exactly the excess charge is located. The reason for the persistent presence of the main resonance in all measured spectra is the smallness of probability of excess/deficient charge(s) capture.

According to the Fluctuation-dissipation theorem, fluctuations of the electrical charge can be calculated as

$$\overline{Q^2} = \frac{\hbar}{\pi}\int \chi''(\omega)\coth\frac{\hbar\omega}{2T}d\omega, \tag{16}$$

where χ'' is the imaginary part of the susceptibility $\chi = \chi' + i\chi'' \equiv Q/U$ of the charge with respect to the applied voltage U because voltage is the energetically conjugated force to the charge, $E = QU$ [22]. The fundamental Fluctuation-dissipation theorem is most known for its application to the noise of the current through a resistor. The imaginary susceptibility to the periodical force $U = U_0\cos\omega t$ is $\chi''(\omega) = 1/\omega R$. The spectral density of charge fluctuations is thus $d\overline{Q^2}/d\omega = (\hbar/\pi R\omega)\cdot\coth\hbar\omega/2T$, and the spectral density of the current is $d\overline{I^2}/d\omega = 1/(\pi R)\hbar\omega\coth\hbar\omega/2T$. At high temperatures $\coth\hbar\omega/2T = 2T/\hbar\omega$ which gives the famous Nyquist formula, $d\overline{I^2}/d\omega = 2T/\pi R$, while at low temperatures, $T \ll \hbar\omega$, $\coth\hbar\omega/2T \to 1$, and the spectral density of current noise is $d\overline{I^2}/d\omega = \hbar\omega/\pi R$ [18].

More generally, a nanotube, as well as other nanomechanical oscillators, presents a LCR-circuit. Charge fluctuations of the capacitance can be calculated similarly to the above

calculations of a pure resistive sample. The generalized susceptibility for a LCR-circuit is $\chi''(\omega) = R\omega[\Lambda^2(\omega^2 - \omega_0^2)^2 + R^2\omega^2]^{-1}$, where $\omega_0 = 1/\sqrt{\Lambda C}$ and Λ denoting the inductance. The inductance of the nanotube with radius $r_0 = 0.8$ nm, length $L = 700$ nm and distance $H = 300$ nm from the gate is $\Lambda \simeq (\mu_0 L/2\pi) \ln H/r_0 = 8.3 \cdot 10^{-13}$ H. With the capacitance $C = 2\pi\varepsilon_0 L/\ln(2H/r_0) = 5.9 \cdot 10^{-18}$ F we obtain the resonant angular frequency $\omega_0 \approx 5 \cdot 10^{14}$ rad/s. For a typical resistance R of 300 kOhm the high frequency cutoff is determined by the lowest cutoff $\omega_c = \omega_{RC} = (RC)^{-1} \approx 5 \cdot 10^{11}$ rad/s $\ll \omega_0$, while $\omega_{LR} = R/\Lambda \approx 4 \cdot 10^{17}$ rad/s $\gg \omega_0 \gg \omega_{RC}$.

The high-frequency cutoff ω_{RC} corresponds to ~ 4 Kelvin. The charge fluctuations below 1 K are therefore

$$\overline{Q^2_{LCR}} = \frac{\hbar R}{\pi} \int_0^{\omega_{RC}} \frac{\omega d\omega}{\Lambda^2(\omega^2 - \omega_0^2)^2 + R^2\omega^2} \approx \frac{\hbar R}{\pi} \int_0^{\omega_{RC}} \frac{\omega d\omega}{1/C^2 + R^2\omega^2} = \frac{\hbar}{2\pi R} \int_0^1 \frac{d(\omega/\omega_{RC})^2}{1 + (\omega/\omega_{RC})^2} = \frac{\hbar \ln 2}{2\pi R}. \tag{17}$$

Although in the case of a pure resistive sample charge fluctuations diverge even in the quantum limit, $\overline{Q^2} = (\hbar/\pi R) \int d\omega/\omega$, yet any small but finite capacitance converges the integral, albeit is not present in the finite result.

In our sample, the average fluctuation of charge $\sqrt{\overline{Q^2_{LCR}}} \simeq 6 \cdot 10^{-21}$ C is much smaller than the elementary charge $\bar{e}$. Although Eq. (17) was derived for continual, not quantized charge, the value of $\sqrt{\overline{Q^2_{LCR}}}$ can be considered as the average charge in the large set of N similar devices. Restricting ourselves to only single-electron trapping, $\overline{Q^2} = \bar{e}^2(n/N)$, where n is the amount of charged tubes in the set of N. As the averaging over the ensemble is equivalent to averaging over time, an average relative time of presence of excess (missing) electron on every tube is about $t_{ex}/T = \overline{Q^2}/\bar{e}^2 = 0.0015$. The observed probability of the charge fluctuation is indeed on the order of average relative amplitude I_{SP}/I_{main} of the side peak, Fig. 1(f), although a strong dependence of I_{SP}/I_{main} on the RF-drive remains to be explained.

[1] Bretz, M., Dash, J. G., Hickernell, D. C., McLean, E. O. & Vilches, O. E. Phases of ^{3}He and ^{4}He monolayer films adsorbed on basal-plane oriented graphite. *Phys. Rev. A* **8,** 1589–1615

(1973).

[2] Greywall, D. S. Heat capacity of multilayers of ^{3}He adsorbed on graphite at low millikelvin temperatures. *Phys. Rev. B* **41,** 1842–1862 (1990).

[3] Godfrin, H. & Lauter, H.-J. "Experimental properties of ^{3}He adsorbed on graphite", in *Progress in Low Temperature Physics, Volume XIV*, W. P. Halperin Ed. (Elsevier Science B.V., Amsterdam, 1995), pp. 213–320.

[4] Greywall, D. S. Heat capacity and the commensurate-incommensurate transition of ^{4}He adsorbed on graphite. *Phys. Rev. B* **47,** 309–318 (1993).

[5] Sato, D., Naruse, K., Matsui, T. & Fukuyama, H. Observation of self-binding in monolayer ^{3}He. *Phys. Rev. Lett.* **109,** 235306 (2012).

[6] Nyéki, J. et al. Intertwined superfluid and density wave order in two-dimensional ^{4}He, *Nature Physics* **13,** 455–459 (2017).

[7] Nyéki, J., Phillis, A., Cowan, B. & Saunders, J. On the 'supersolid' response of the second layer of ^{4}He on graphite, *J. Low Temp. Phys.* **187,** 475–481 (2017).

[8] Todoshchenko, I. et al. Topologically-imposed vacancies and mobile solid ^{3}He on carbon nanotube, *Nat. Commun.* **13,** 5873 (2022).

[9] Todoshchenko, I. et al. Quantum degeneracy in mesoscopic matter: Casimir effect and Bose-Einstein condensation. *Phys. Rev. B* **109,** 224519 (2024).

[10] Saunders, J., Cowan, B. & Nyéki, J. Atomically layered helium films at ultralow temperatures: model systems for realizing quantum materials *J. Low Temp. Phys* **201,** 615–633 (2020).

[11] Kumashita, A. et al. Growth of uniform helium submonolayers adsorbed on single-surface graphite observed by surface X-ray diffraction. *J. Low Temp. Phys* **220,** 115–123 (2025).

[12] Landau, L. D. & Lifshitz, E. M. *Course of Theoretical Physics, Volume III (Quantum Mechanics)* (Pergamon Press, Oxford, 1969).

[13] Aziz, R. A. & Slaman, M. J. An examination of ab initio results for the helium potential energy curve. *J. Chem. Phys.* **94,** 8047–8053 (1991).

[14] Joly, F., Lhuillier, C. & Brami, B. The helium-graphite interaction. *Surf. Sci.* **264,** 419–422 (1992).

[15] Averin, D. V. & Likharev, K. K. "Single-Electronics", in: *Mesoscopic Phenomena in Solids*, B. Altshuler, P. Lee, and R. Webb Ed. (Elsevier Science Publishers B.V., Amsterdam, 1991), pp. 173–271.

[16] Kaikkonen, J.-P. et al. Suspended superconducting weak links from aerosol-synthesized single-walled carbon nanotubes. *Nano Res.* **13,** 3433–3438 (2020).

[17] Häkkinen, P., Isacsson, A., Savin, A., Sulkko, J. & Hakonen, P. J. Charge sensitivity enhancement via mechanical oscillation in suspended carbon nanotube devices. *Nano Lett.* **15,** 1667–1672 (2015).

[18] Landau, L. D. & Lifshitz, E. M. *Course of Theoretical Physics, Volume IX (Theory of the Condensed State)* (Pergamon Press, Oxford, 1969).

[19] Todoshchenko, I. A., Alles, H., Junes, H. J., Parshin, A. Ya. & Tsepelin, V. Surface of a ^{3}He crystal: Crossover from quantum to classical behavior. *Phys. Rev. Lett.* **93,** 175301 (2004).

[20] Zaliznyak, I. A. Effect of the magnetic field on quantum fluctuations in quazi-one-dimentional hexagonal antiferromagnets. *Solid State Comm.* **84,** 573–576 (1992).

[21] Lassagne, B., Tarakanov, Y., Kinaret, J., Garcia-Sanchez, D. & Bachtold, A. Coupling mechanics to charge transport in carbon nanotube mechanical resonators, *Science* **325,** 1107–1110 (2009).

[22] Landau, L. D. & Lifshitz, E. M. *Course of Theoretical Physics, Volume V (Statistical Physics)* (Pergamon Press, Oxford, 1969).